Discovery and structure–activity relationship of 2-phenyl-oxazole-4-carboxamide derivatives as potent apoptosis inducers

Vincent W.-F. Tai,[a],* David Sperandio,[a] Emma J. Shelton,[a] Joane Litvak,[a] Keith Pararajasingham,[a] Ben Cebon,[a] Julia Lohman,[a] John Eksterowicz,[a] Seema Kantak,[a] Peter Sabbatini,[a] Cindy Brown,[a] Jennifer Zeitz,[a] Chris Reed,[a] Bill Maske,[a] Doris Graupe,[a] Alberto Estevez,[a] Jason Oeh,[a] Darren Wong,[a] Yong Ni,[a] Paul Sprengeler,[a] Robert Yee,[a] Catherine Magill,[a] Anthony Neri,[a] Sui Xiong Cai,[b] John Drewe,[b] Ling Qiu,[b] John Herich,[b] Ben Tseng,[b] Shailaja Kasibhatla[b] and Jeffrey R. Spencer[a],*

[a]Celera Genomics, 180 Kimball Way, South San Francisco, CA 94080, USA
[b]EpiCept Corporation, 6650 Nancy Ridge Drive, San Diego, CA 92121, USA

Abstract—As a continuation of our efforts to discover novel apoptosis inducers as anticancer agents using a cell-based caspase HTS assay, 2-phenyl-oxazole-4-carboxamide derivatives were identified. The structure–activity relationships of this class of molecules were explored. Compound **1k**, with EC_{50} of 270 nM and GI_{50} of 229 nM in human colorectal DLD-1 cells, was selected and demonstrated the ability to cleave PARP and displayed DNA laddering, the hallmarks of apoptosis. Compound **1k** showed 63% tumor growth inhibition in human colorectal DLD-1 xenograft mouse model at 50 mpk, bid.
© 2006 Elsevier Ltd. All rights reserved.

Apoptosis, or programmed cell death, is central to a number of physiological processes and is essential for animal development as well as tissue homeostasis.[1,2] Recent efforts in this field have identified multiple signaling cascades leading to cell death. Two major mechanisms are involved in the induction of apoptosis: agents that activate a family of death receptors leading to the activation of the apoptotic cascade; or agents that trigger the release of cytochrome C from mitochondria followed by apoptosis. Both mechanisms lead to the activation of caspases, a group of cysteine proteases, which carry out the cleavage of both structural and functional elements of the cell.[3] This results in morphological changes such as cellular shrinkage, chromatin condensation, membrane blebbing, and fragmentation into membrane-enclosed vesicles.

It has been demonstrated that various anticancer agents cause apoptosis in cancer cells;[4,5] therefore, the rapid identification of structurally diverse apoptosis inducers offers a novel approach in the discovery of new anticancer agents. A cell-based high-throughput screen tracking the activation of endogenous caspase-3 was previously reported[6–8] and employed for this purpose. Herein, we report the discovery and structure–activity relationships (SAR) of a new class of 2-aryl-oxazole-4-carboxamide-containing apoptosis inducers and their in vivo activities.

A panel of three different human cancer cell lines was used for the HTS assays. Briefly, human breast cancer cell lines T47D, ZR751 and human colorectal cancer cell line DLD-1 were plated in 384-well microtiter plates containing various concentrations of test compound and incubated at 37 °C for 24 h. After incubation, the samples were treated with fluorogenic substrate N-(Ac-DEVD)-N-ethoxycarbonyl-R110[9] and incubated for 3 h. The caspase activation activity (EC_{50}) was determined by sigmoidal dose–response calculation.[10] Compound **1a** was found to activate caspases and induce apoptosis with EC_{50} values of 0.55, 0.29, and 0.92 μM in T47D, ZR751, and DLD-1 cells, respectively. In this report, we will focus on the colorectal DLD-1 cell line

since we have successfully developed a DLD-1-implant-ed xenograft mouse model.
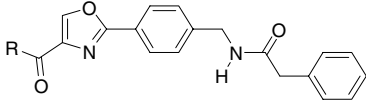

1a
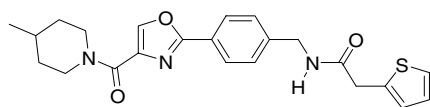
EC$_{50}$ T47D = 0.55 μM
EC$_{50}$ ZR751 = 0.29 μM
EC$_{50}$ DLD1 = 0.92 μM

Synthesis of 2-phenyloxazole scaffold was optimized as shown in Scheme 1. Coupling of serine methyl ester hydrochloride (**2**) and commercially available 4-{[(*tert*-butoxycarbonyl)amino]methyl}benzoic acid (**3**) under EDC/HOBt condition gave ester **4** in 90% yield.[11] Treatment of ester **4** with Burgess reagent induced cyclodehydration to give oxazoline which was oxidized with CBrCl$_3$/DBU to give oxazole **5**.[12,13] Alternatively, conversion of **4** to **5** can be carried out using Williams' protocol [(diethylamino)sulfur trifluoride (DAST)][14] followed by oxidation. Ester **5**, substituted with orthogonal protecting groups at the amino and carboxylic acid groups, is a versatile intermediate for the SAR studies of amides at positions A and D. In route A, the Boc protecting group was cleaved readily with 4 M hydrochloric acid in dioxane/CH$_2$Cl$_2$ followed by coupling with an acid to give amide **7**. The methyl ester was then saponified with lithium hydroxide in THF/H$_2$O mixture followed by the coupling with various substituted cyclic amines. This approach allowed rapid optimization of cyclic amines at position A. Alternatively, optimization of acyl group at position D can be carried out as illustrated in route B using similar reaction conditions.

To study the SAR of cyclic amines at position A, a more potent phenylacetyl group was chosen at position D (see below). As shown in Table 1, cyclic amino substitution at position A showed an interesting trend as potency peaks at the 7-membered homopiperidine ring. An interesting correlation between the potency (EC$_{50}$) of the compounds and the van der Waals volume of the molecules was observed (Fig. 1). The similar potency of 2,5-dimethylpyrrolidine **1f** and homopiperidine **1g** can be explained using this model as they have similar van der Waals volumes. The piperidine and homopiperidine rings were selected for further substitution and the

Table 1. SAR studies at position A

Compound	Cyclic amines R	Ec$_{50}$DLD-1 (nM)
1b		553
1c		318
1d		108
1e		65
1f		34
1g		33
1h		108
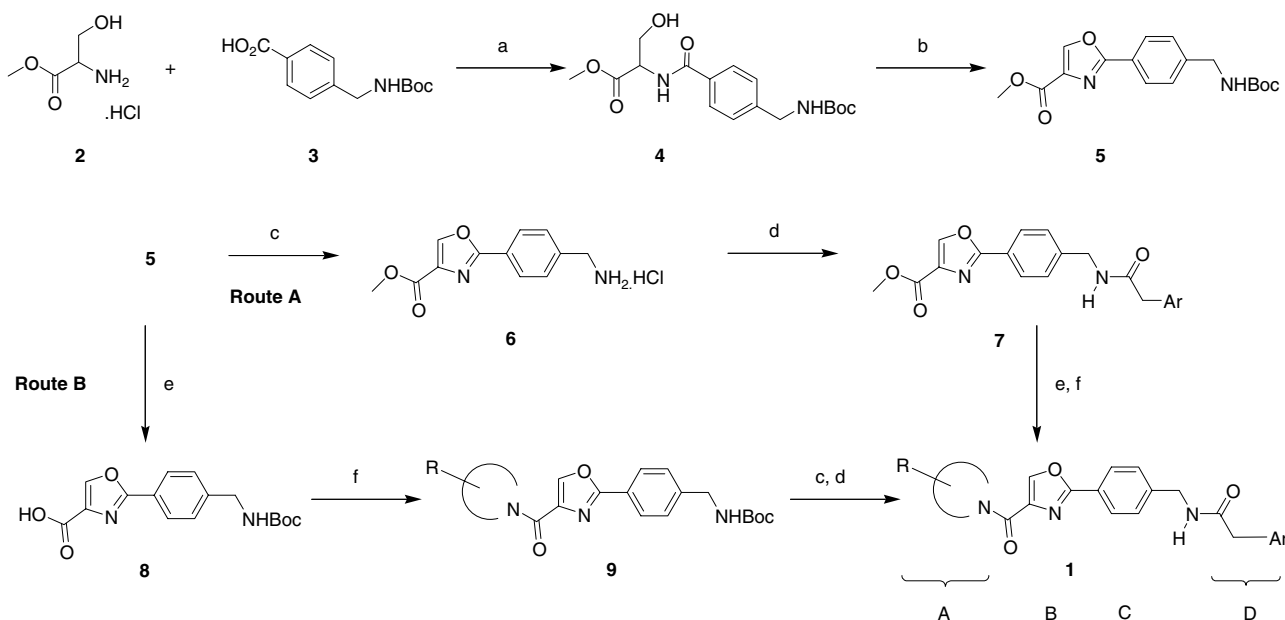
Scheme 1. Reagents and conditions: (a) EDC, HOBt, ^{i}Pr$_2$NEt, DMF (90%); (b) i—Burgess reagent (MeO$_2$CN$^-$SO$_2$N$^+$Et$_3$), 60 °C, 2 h; or DAST, CH$_2$Cl$_2$, −78 °C (80–90%); ii—CBrCl$_3$, DBU, CH$_2$Cl$_2$ (73%); (c) HCl, dioxane, CH$_2$Cl$_2$ (90–100%); (d) acid, EDC, HOBt, ^{i}Pr$_2$NEt, DMF (70–85%); (e) LiOH, THF, H$_2$O (85–95%); (f) cyclic amine, PyBOP, ^{i}Pr$_2$NEt, DMF (65–80%).
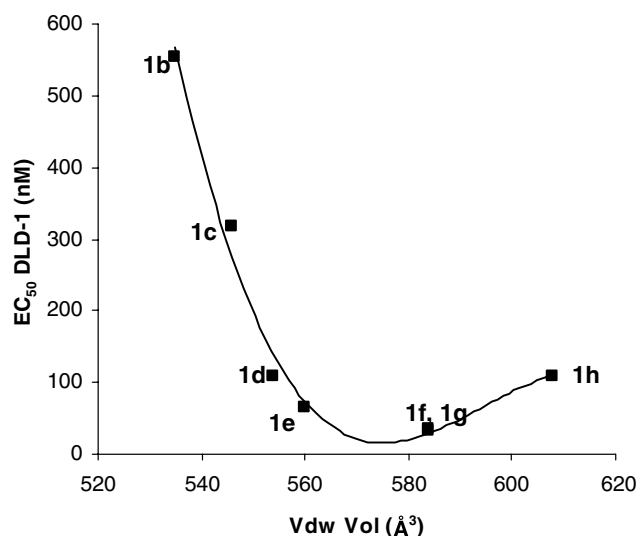
Figure 1. A plot of EC_{50} (DLD-1) versus van der Waals Å volume that was calculated using a grid approximation (spacing 0.75 Å).[15]

results of the piperidine substitutions are reported in Table 2.

Substitutions at both the 3- and 4-positions of the piperidine ring resulted in loss of potency relative to **1e** with the exception of 3,3-difluoropiperidine **1i** (EC_{50} = 20 nM). Halogen substitutions in general are more tolerated at the 3-position than at the 4-position. On the other hand, compounds with oxygen-containing substituents such as the hydroxyl, keto-, and hydroxymethyl- were more potent than the halo-substitutions at the 4-position. Despite losing some potency compared to **1e**, these oxophilic compounds showed better water solubility compared to the parent compound **1e**.

Using the unsubstituted piperidine amide as in analog **1e**, the SAR at position D was explored. The linker between the amide and the aromatic group was first elaborated (Table 3). It is interesting to note that the optimal spacer of a single methylene unit is the outcome from the HTS campaign. Phenyl, 2-thienyl, 2-furanyl groups gave similar potency (EC_{50} < 100 nM), while pyridines and 3-methyl isoxazole ring substitutions were detrimental to caspase-3 activation activity. Substitution on the phenyl ring in general does not improve potency compared to the parent compound **1e** but offers a handle for optimizing other physical properties such as solubility. It is noteworthy that fluoro substitution is more tolerated at the 2- and 3-positions, while the hydroxyl group is more tolerated at the 4-position.

Selected compounds were also tested by an in vitro growth inhibition (GI_{50}) assay to confirm that the active compounds can inhibit tumor cell growth.[10] As shown in Table 4, compound **1i** is one of the most potent compounds in this scaffold. In general, compounds that are more potent in the apoptosis induction assay, as measured by caspase activation, are also more potent in the growth inhibition assay.

Compound **1k** was selected for further biological studies. Caspase-mediated cleavage of the DNA-repair enzyme PARP (poly-ADP-ribose polymerase) was

Table 2. SAR of substituted piperidine ring at position A

Compound	R	EC_{50} DLD-1 (nM)
1i	3-F	85
	3,3-F,F	20
	3-Cl	119
	3-Me	193
	3-OH	196
	3-OMe	259
	3-(O)	235
	4-F	304
	4,4-F,F	979
	4-Cl	492
	4-Me	258
	4-OH	150
	4-OMe	5229
	4-(O)	115
	4-CH₂OH	196

Table 3. SAR studies at position D

Compound	R	EC_{50} DLD-1 (nM)
	2-Thienyl	>10,000
1j	–CH₂(2-Thienyl)	59
	–(CH₂)₂(2-Thienyl)	487
	–(CH₂)₃(2-Thienyl)	1080
	–CH₂(2-Furanyl)	90
	–CH₂(3-Methyl-isoxazol-5-yl)	2594
	–CH₂(3-Pyridyl)	3315
	–CH₂(2-Pyridyl)	3565
1e	–CH₂Ph	65
	–CH₂(2-F)Ph	65
	–CH₂(2-OH)Ph	1006
	–CH₂(3-F)Ph	72
	–CH₂(3-Cl)Ph	533
	–CH₂(3-OH)Ph	139
	–CH₂(4-F)Ph	233
	–CH₂(4-Cl)Ph	274
	–CH₂(4-OH)Ph	73
	–CH₂(4-Me)Ph	142
1k	–CH₂(4-OCF₃)Ph	270

Table 4. Comparison of caspase activation activity and growth inhibition activity of selected compounds in DLD-1 cells

Compound	EC_{50} DLD-1 (nM)	GI_{50} DLD-1 (nM)	Solubility (µM)
1e	65	258	47
1i	20	15	<10
1j	59	75	29
1k	270	229	44

V. W.-F. Tai et al. / Bioorg. Med. Chem. Lett. 16 (2006) 4554–4558

4557

demonstrated as shown in Figure 2A. PARP cleavage of compound **1k**-treated cells was demonstrated at 48 h using Western blot analysis, whereas untreated control did not show PARP cleavage. Figure 2B shows the DNA laddering of compound **1k**-treated cells after 48 h.

Based on its good caspase activation potency, proliferation assay, solubility, and pharmacokinetic profile, compound **1k** was evaluated in human tumor xenograft models. At once a day dosing, compound **1k** showed 21% ($p = 0.096$) and 38% ($p = 0.002$) tumor growth inhibition of colorectal DLD-1 tumor xenografts at 50 mpk and 100 mpk, respectively. At 50 mg/kg twice a day, compound **1k** achieved 63% ($p < 0.001$) tumor growth inhibition. No significant weight loss was observed in the above doses (Fig. 3).

In summary, a new class of apoptosis inducers with a 2-phenyl-oxazole-4-carboxamide scaffold was identified through a cell-based caspase HTS assay. SAR studies at position A revealed an interesting correlation between the van der Waals volume of the molecule with caspase activation in one subgroup of analogs. A strong preference for 6- and 7-membered cyclic amides at position A was found and 3,3-difluoropiperidine-substitution was

determined to be superior at this position. At position D, a single methylene unit was determined to be the best spacer between the aryl/heteroaryl group and the amide group. Replacement of the 2-thienyl group with 2-furanyl or substituted phenyl groups is tolerated. Compound **1k** was further shown to cleave PARP and displayed DNA laddering pattern, the hallmarks for apoptosis. This compound showed tumor growth inhibition in human colorectal DLD-1 xenograft models. Additional biological characterization of this class of compounds will help to understand the mechanism of action of these compounds and improve the efficacy in the future.

Acknowledgments

Figure 2. (A) Cleavage of PARP;[16] The uncleaved PARP is approximately 115 kDa and the caspase-mediated cleavage product (arrow) migrates at approximately 85 kDa. (B) DNA fragmentation of DLD-1 cells.[17] Lane 1, untreated control; lane 2, DLD-1 cells treated with **1k**; lane 3, DLD-1 cells treated with vinblastine.

Figure 3. Anti-tumor activity of compound **1k**-treated athymic female mice bearing DLD-1 human colon tumors.[18] Twelve days post implant of DLD-1 cells, mice were treated with various doses of compound **1k** on days 1–5, 8–12, and 15.

References and notes

1. Lowe, S. W.; Lin, A. W. *Carcinogenesis* **2000**, *21*, 485.
2. Reed, J. C.; Tomaselli, K. J. *Curr. Opin. Biotechnol.* **2000**, *11*, 586.
3. Earnshaw, W. C.; Martins, L. M.; Kaufmann, S. H. *Annu. Rev. Biochem.* **1999**, *68*, 383.
4. Arends, M. J.; Wyllie, A. H. *Int. Rev. Exp. Pathol.* **1991**, *32*, 223.
5. Rich, T.; Allen, R. L.; Wyllie, A. H. *Nature* **2000**, *407*, 777.
6. Zhang, H.-Z.; Drewe, J.; Tseng, B.; Kasibhatla, S.; Cai, S. X. *Bioorg. Med. Chem* **2004**, *12*, 3649.
7. Zhang, H.-Z.; Kasibhatla, S.; Wang, Y.; Herich, J.; Huastella, J.; Tseng, B.; Drewe, J.; Cai, S. X. *Bioorg. Med. Chem.* **2004**, *12*, 309.
8. Zhang, H.-Z.; Kasibhatla, S.; Kuemmerle, J.; Kemnitzer, W.; Ollis-Mason, K.; Qiu, L.; Crogan-Grundy, C.; Tseng, B.; Drewe, J.; Cai, S. X. *J. Med. Chem.* **2005**, *48*, 5215.
9. Zhang, H.-Z.; Kasibhatla, S.; Guastella, J.; Tseng, B.; Drewe, J.; Cai, S. X. *Bioconjugate Chem.* **2003**, *14*, 458.
10. For detailed description of EC_{50} and GI_{50} calculations: Cai, S. X.; Nguyen, B.; Jia, S.; Herich, J.; Guastella, J.; Reddy, S.; Tseng, B.; Drewe, J.; Kasibhatla, S. *J. Med. Chem.* **2003**, *46*, 2474.
11. All new compounds are characterized by ^{1}H NMR and HPLC-MS analyses. Compound **1k**: ^{1}H NMR (400 MHz, DMSO-d_6) δ 1.51–1.68 (m, 6H), 3.55 (s, 2H), 3.58 (br s, 2H), 3.82 (br s, 2H), 4.35 (d, 2H, $J = 5.6$ Hz), 7.29 (br d, 2H, $J = 8$ Hz), 7.35–7.44 (m, 4H), 7.91 (dd, 2H, $J = 1.6$, 8.4 Hz), 8.56 (d, 1H, $J = 2.4$ Hz), 8.68 (t, 1H, $J = 5.6$ Hz); MS (ES) m/z 488.1 (MH+); MS calcd: 487.2 (M).
12. Wipf, P.; Miller, C. P. *Tetrahedron Lett.* **1992**, *33*, 907.
13. Williams, D. R.; Lowder, P. D.; Gu, Y.-G.; Brooks, D. A. *Tetrahedron Lett.* **1997**, *38*, 331.
14. Philips, A. J.; Uto, Y.; Wipf, P.; Reno, M. J.; Williams, D. R. *Org. Lett.* **2000**, *2*, 1165.
15. MOE, Molecular Operating Environment; 2005.06; Chemical Computing Group, Inc., Montreal, Canada, 2005.
16. PARP cleavage—DLD-1 cells were seeded at 10^6 cells per 10-cm dish and 24 h later were treated with compound **1k** (1 μM) or vinblastine (400 nM) (final concentration of DMSO was 0.2%). After 48 h, cells were harvested and whole-cell lysates prepared using standard procedures. Cell extract (30 μg) was electrophoretically separated on a
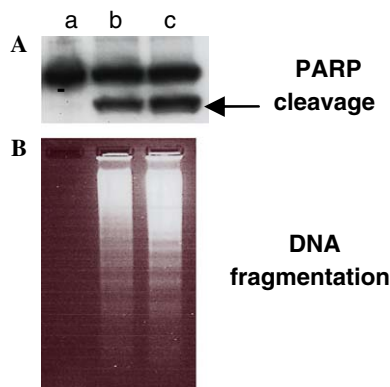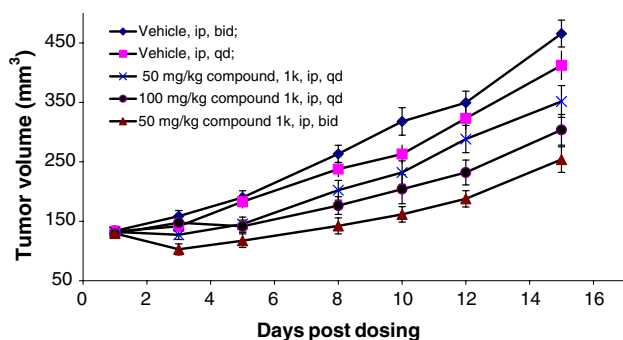
4–20% Tris–glycine gel (Novex), blotted, and hybridized overnight with anti-PARP polyclonal antibody (cell signaling, Inc.). After subsequent washing and hybridization with HRP-anti-rabbit secondary antibody, proteins were detected using enhanced chemiluminescence according to the manufacturer's instructions.

17. DNA fragmentation analysis—DLD-1 cells were seeded at 10^6 cells per 10-cm dish and 24 h later were treated with compound **1k** (1 μM) or vinblastine (400 nM). After 48 h, the cells were harvested by trypsinization, washed with PBS (pH 7.4), and lysed in Triton X buffer (0.2% Triton X-100, 10 mM Tris, and 10 mM EDTA). After 10 min incubation on ice, lysates were pelleted and supernatant extracted twice with phenol/chloroform using standard procedures. Small MW DNA was then precipitated with 300 mM NaCl and ethanol at −80 °C. Precipitates were then lyophilized, resuspended in Tris/EDTA containing 0.6 mg/mL RNASe, and incubated at 37 °C for 30 min. Samples were then electrophoresed on a 2% TAE gel containing ethidium bromide and visualized under ultraviolet light.

18. In vivo assays—female Balb/c nude mice (8–10 weeks old, Jackson Lab) were implanted with 3×10^6 DLD-1 cells resuspended in serum-free media containing 50% matrigel (BD Biosciences). Twelve days postimplant, when tumors reached 100–150 mm^3, the mice were randomized into treatment groups and treated with compound **1k**. All animals were weighted daily, and caliper measurements were taken three times a week after tumors were calculated by the Mann–Whitney rank sum test using SigmaStat software. Two-sided *p*-values are given at a 95% confidence level.